

# A hidden Markov model for disease interactions

Chris Sherlock<sup>1</sup>, Tatiana Xifara<sup>1\*</sup>, Sandra Telfer<sup>2</sup>,  
Mike Begon<sup>3</sup>

<sup>1</sup> *Department of Mathematics and Statistics, Lancaster University, UK*

<sup>2</sup> *Institute of Biological and Environmental Sciences, University of Aberdeen, UK*

<sup>3</sup> *Institute of Integrative Biology, University of Liverpool, UK*

5 March 2012

## Abstract

To investigate interactions between parasite species in a host a population of field voles was studied longitudinally with presence or absence of six different parasites measured repeatedly. Although trapping sessions were regular, a different set of voles was caught at each session leading to incomplete profiles for all subjects. A simple analysis, which discards much of the data, has already been carried out; we offer a more powerful alternative. We use a discrete-time hidden Markov model for each disease with transition probabilities dependent on covariates via a set of logistic regressions. For each disease the hidden states for each of the other diseases at a given time point form part of the covariate set for the Markov transition probabilities from that time point. This allows us to gauge the influence of each parasite species on the transition probabilities for each of the other parasite species. Inference is performed via a Gibbs sampler, which cycles through each of the diseases, first using an adaptive Metropolis-Hastings step to sample from the conditional posterior of the covariate parameters for that particular disease given the hidden states for all other diseases and then sampling from the hidden states for that disease given the parameters.

**Keywords:** Adaptive MCMC, Forward-Backward algorithm, Gibbs sampler, HMM, zoonosis.

## 1 Introduction

### 1.1 Motivating problem

In natural populations, animals are likely to be infected by a variety of pathogens, either simultaneously or successively. Interactions between these pathogens,

---

\*Correspondence author: t.xifara@lancaster.ac.uk, Department of Mathematics and Statistics, Lancaster University, UK

which can be synergistic or antagonistic, can affect infection biology (e.g. the intensity of one or both infections), host susceptibility to infection, or may impact on the host’s morbidity or/and mortality. However, the biological processes involved are often too complex to allow clear-cut predictions regarding the outcome of such interactions. In order to explore potential interactions, a longitudinal study was undertaken by recording the sequences of infection events for different parasites in four spatially distinct populations of field voles (*Microtus agrestis*). The data are records of six pathogens: three species of *Bartonella* bacteria (*B. taylorii*, *B. grahamii*, *B. doshiae*), cowpox virus, the bacterium *Anaplasma phagocytophilum* and the protozoan *Babesia microti*. Aside from their intrinsic interest as a community of pathogens, *Bartonella*, *Anaplasma*, *Babesia* and cowpox virus infections may all also be zoonotic: capable of being transmitted from animals to humans and causing disease.

As in most capture-mark-recapture studies, a different set of voles was caught at each session leading to incomplete profiles for all subjects. The dataset therefore contains many missing observations; for example a profile for a given vole and a given disease from the first to last observation times for that vole might be  $NPxxPNxP$ , where  $x$ ,  $N$  and  $P$  respectively indicate a missing observation, a negative response and a positive response. Inference on incomplete data in longitudinal and capture-recapture studies is a major problem; for examples see Daniels and Hogan (2008) and Pradel (2005). Previous analyses of our and related datasets were limited as they discarded much of the dataset (see Telfer *et al.* (2010), Begon *et al.* (2009), and Section 1.3). In this paper we offer a more realistic model and a more powerful analysis methodology for investigating the effects of previous infections for each disease on the other diseases. We use a hidden Markov model for each disease (Section 3.1) and perform inference via a Gibbs sampler; this allows us to infer covariate effects on a given disease, even when these covariates are the (potentially missing or hidden) states of the other five diseases.

## 1.2 Data

We utilize a set of data collected between March 2005 and March 2007 from field voles in Kielder Forest, a man-made forest on the English-Scottish border. The voles were trapped at four grassy clear-cut sites within the forest, with each site at least 3.5km from the nearest neighbouring site. Specifically, the Kielder catchment included Kielder Central Site (KCS) and Plashett’s Jetty (PLJ) and was approximately 12 km from Redesdale catchment, where Black Blake Hope (BHP) and Rob’s Wood (ROB) were situated. Individuals were trapped within a 0.3ha live-trapping grid comprising 100 traps set at 5m intervals, with trapping taking place every 28 days from March to November, and every 56 days from November to March. Begon *et al.* (2009) provides further details of the study area and the trapping design. A brief description of the observed and derived variables is given in Table 1.

Captured voles were marked with a unique identifying passive transponder tag in order to be recognized in later captures. At each capture, a 20 – 30 $\mu$ l

Table 1: Description of variables in the data set and their possible outcomes

<i>Variable</i>	<i>Description</i>
Tag	Unique number that identifies each vole
Site	One of four sites: BHP, LCS, PLJ and ROB
Sex	Male, Female
Lm	Capture time point in whole lunar months (1 - 27, integer)
Weight	Weight in grams rounded to the nearest 0.5g
SeasSin	$\sin(2\pi lm/13)$
SeasCos	$\cos(2\pi lm/13)$
Tay	<i>B. taylorii</i> , N(negative) or P(positive)
Grah	<i>B. grahamii</i> , N(negative) or P(positive)
Dosh	<i>B. doshiae</i> , N(negative) or P(positive)
Cow	Cowpox, N(negative) or P(positive)
Ana	<i>Anaplasma</i> , N(negative) or P(positive)
Bab	<i>Babesia</i> , N(negative) or P(positive)

blood sample was taken for pathogen diagnostic tests. Previously described PCR assays were used to directly test for evidence of infection with *Anaplasma phagocytophilum*, *Babesia microti* and the three *Bartonella* spp. (see Courtney *et al.* (2004), Bown *et al.* (2008) and Telfer *et al.* (2008)). Antibodies to cowpox virus were detected by immunofluorescence assay (see Chantrey *et al.* (1999)).

### 1.3 Inference on a subset of the data using a simple model

In this section we describe a simple analysis that uses a similar approach to those used in Telfer *et al.* (2010) and Begon *et al.* (2009) to analyse a larger but less detailed dataset. Firstly this provides evidence that there are interactions between the diseases and justifies our main analysis. Secondly it allows us to decide upon a sensible set of non-disease covariates to carry forward to our main analysis. Finally it provides a baseline to which we can compare our methodology and results.

For each disease,  $D$ , the approach used here considers voles that are free of  $D$  at a given observation time,  $t_0$ , and examines the influence of a set of covariates, which includes presence or absence of the other diseases and which are observed at this time, on the probability that the vole will have contracted  $D$  by time  $t_1$ , which for this data set is exactly one lunar month after  $t_0$ . The covariate set for this model consists of all variables in Table 1 except for the disease which is currently the response. As will be discussed in Section 3.1 both the cowpox and *B. microti* covariates were turned in to 3 level factors. This allows us to distinguish between new infections (first month positive) and chronic infections (also positive previously) of *B. microti*, since voles may remain infected for extended periods. For cowpox virus, it allows us to distinguish between voles that currently have cowpox (first month positive) and those that have had it in

the past (also positive previously), since voles only remain infected for around one month, but recovered voles are likely to retain detectable levels of antibody for the rest of their lives.

For a given disease and for each vole the analysis considers all pairs of observations that are one lunar month apart and for which the first observation is  $N$ . It is assumed that the disease status of each vole does not affect the probability of it being captured. This has been supported in the case of cowpox virus (Burthe *et al.* (2008)) and is equally believable for the other infections since no overt symptoms have ever been described in field voles for any of these infections. A logistic regression is fitted separately for each disease. As well as a variety of covariate effects, each regression model is also allowed to include a subject specific random intercept and a different random intercept for each lunar month at each site. When considering models with both sets of random effects, the numerical integration was performed via the Laplace approximation used by Lindley (1980). Models were fitted using the functions `glmer()` and `glm()` in R (?) and since many of the models are not nested they are compared via Akiake's Information Criterion (AIC) (e.g. Pawitan (2001)).

The best fitting models do include some disease interactions. Specifically *Babesia* reduces susceptibility to infection with all *Bartonella* spp.; the reduction to susceptibility to infection of *B. grahamii* for individuals with chronic *Babesia* infections is especially pronounced. In addition, presence of cowpox antibodies, indicative of a recovered state, decreases the probability of contracting *B. taylorii* and there is evidence for the same interaction with *B. doshiae*. For interactions amongst *Bartonella* spp., animals with *B. taylorii* infections are more likely to become infected with *B. grahamii*. Finally, there is evidence that *B. grahamii* infections are associated with increased susceptibility to *Babesia*. These results justify the choice to distinguish in our complicated models the three species of *Bartonella* both as covariates and as dependent variables. This distinction has not been considered in previous analyses. Furthermore it justifies the need to distinguish between the two categories of animals that are uninfected by cowpox: those that have never been infected and those that have recovered from a past infection.

The best final model for cowpox contains a different trend with lunar month for each site, with a reduction in AIC of 27 compared to the best model without these trends. For each disease the best model required no random effects, neither a subject specific random intercept nor a different random effect for each lunar month at each site.

The best models also suggest a clear effect of seasonal covariates on the probability of contracting all diseases, except for *B. doshiae* (see also, e.g. Telfer *et al.* (2010)). Differences between sexes appear to be important for *Babesia* and *Anaplasma*, to which males are more susceptible, and for some the interaction between sex and seasonal cycle.

## 1.4 Statistical challenges

The dataset contains a substantial fraction of missing data: most voles are not captured at every lunar month between the first and last times they were observed. Thus, even for many of the voles that were observed at least twice, not all of the covariates are available, either because the vole was not caught in a given lunar month, or sometimes because the vole was caught but a given variable was not ascertained.

We aim to investigate potential interactions between the six pathogens of the study. In particular, for each disease,  $D$ , we wish to evaluate the way in which the presence or absence of each of the other diseases (and perhaps further information such as whether or not any infection is in its first month) affects the probability of a vole contracting  $D$ . Additionally where applicable we are interested in how other diseases affect the probability of recovery from  $D$ .

We aim to describe the evolution of each disease within a vole using a discrete-time Markov model. The simplest model would have two states which correspond to absence and presence of the infection, but for many of the diseases we will in fact require three or four states in order to adequately describe the dynamics of the disease (see Section 3.1).

Pradel (2005) analyses capture-recapture data using a hidden Markov model (HMM), and incorporation of covariate information within this framework via an appropriate link function is straightforward (see for example Lachlish *et al.* (2011)). However the methodology does not allow the use of multiple HMMs nor, therefore, can it use the state of each HMM as a covariate for the other HMMs. We require six HMMs (one for each disease) and we wish to use covariate information such as the time of year and weight of the vole. Furthermore we wish the covariate set for each disease to include the states of the HMMs for the other diseases. In essence, for each disease,  $D$ , we will represent the probability of each possible state change through a logistic regression. However some of the covariates, the states of the other HMMs, are unknown. Our solution is a Gibbs sampler which employs the forward-backward algorithm and adaptive random walk Metropolis steps to jointly sample from the true posterior distribution of all of the HMMs and the covariate parameters.

## 1.5 Outline

The remainder of this paper is organised as follows. In Section 2 we outline the forward-backward algorithm and the adaptive random walk Metropolis-Hastings algorithm (RWM), both of which are used in our Gibbs sampler. Section 3 describes the model which was used for each disease, and the imputation of the missing weight values and the other fixed values. The Markov chain Monte Carlo algorithm is described in Section 4 and we present our results, including the sensitivity study, in Section 5. The paper concludes with a discussion.

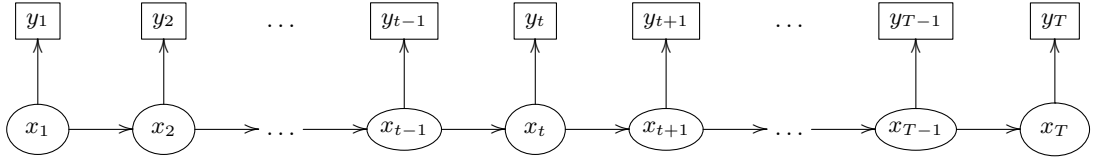


Figure 1: Directed graph of a hidden Markov model; where  $y_t$ ,  $t = 1, \dots, T$ , are the observed values and  $x_t$ ,  $t = 1, \dots, T$ , are the states of the hidden Markov chain.

## 2 Forward-backward and adaptive RWM algorithms

### 2.1 The forward-backward algorithm

The forward-backward algorithm developed by Baum *et al.* (1970) provides us with two useful tools. Its first part evaluates the likelihood, while the second part allows us to simulate from the distribution of the hidden states of the Markov chain given the observed data.

In a hidden Markov model (HMM), let  $\mathbf{X}_T := (X_1, X_2, \dots, X_T)$  be the unobserved Markov chain of cardinality  $n$ , with transition probability matrix  $\mathbf{P}$  and initial distribution  $\pi$ . Let  $\mathbf{Y}_T := (Y_1, Y_2, \dots, Y_T)$  be the observed process, where  $Y_i$  is conditionally independent of  $X_1, \dots, X_{i-1}, X_{i+1}, \dots, X_T$  given  $X_i$ . These two processes have two significant dependence properties, shown in Figure 1.

By definition, in a HMM the states of the Markov chain are not observable and the observations are probabilistic functions of the states. Denoting the conditional distribution of  $Y_t$  by  $l_i^{(t)} := l_i(y_t) = P(Y_t = y_t | X_t = i)$ ,  $i = 1, \dots, n$ , we may define the likelihood vector  $\mathbf{l}^{(t)} = (l_1^{(t)}, l_2^{(t)}, \dots, l_n^{(t)})$ . Let  $\mathbf{Y}_t := [Y_1, \dots, Y_t]^t$  and  $\mathbf{X}_t := [X_1, \dots, X_t]^t$  respectively denote the observed and unobserved sequences up to time  $t$ .

The *forward recursion* provides a computationally efficient algorithm for calculation the likelihood of the observed data. It uses the joint probability of the observed sequence up to time  $t$ ,  $(y_1, \dots, y_t)$ , and the state,  $x_t$ , of the unobserved Markov chain at this time  $t$ . From the conditional dependence structure of the model

$$P(y_{1:t}, x_t) = \sum_{x_{t-1}} P(y_{1:t} | x_t) P(x_t | x_{t-1}) P(y_{1:t-1}, x_{t-1}).$$

The first step of the recursion calculates  $P(y_1, X_t = i) = \pi_i l_i^{(1)}$  and the final step creates  $P(y_{1:T}, x_T)$ ,  $x_T = 1, \dots, n$ . So, we can calculate the likelihood of the observed data via the following summation

$$P(y_1, \dots, y_T) = \sum_{x_T} P(y_{1:T}, x_T),$$

the complexity of which is just  $O(T)$  calculations. Thus by using the forward algorithm the complexity of the likelihood's calculation is  $O(n^2T)$ , which is much smaller than the  $O(n^T)$  steps required for the naive summation of the complete data likelihood,  $P(x_{1:T}, y_{1:T})$ , over all possible combinations of  $x_{1:T}$ .

The *backward algorithm* enables us to simulate the states of the hidden Markov chain. This can be accomplished by calculating backwards the conditional probability of the state of the hidden Markov chain at time  $t$  given the observed data and the hidden state at time  $t + 1$ . Again, from the conditional dependence structure of the model,

$$P(x_t | y_{1:T}, x_{(t+1):T}) = P(x_t | y_{1:t}, x_{t+1}) = \frac{P(x_{t+1} | X_t) P(y_{1:t}, X_t)}{\sum_{X_t} P(x_{t+1} | X_t) P(y_{1:t}, x_t)}. \quad (1)$$

We may therefore simulate first the final state of the Markov chain,  $x_T$ , by

$$P(x_T | y_{1:T}) = \frac{P(y_{1:T}, x_T)}{P(y_{1:T})},$$

and, since  $P(y_{1:t}, x_t)$  has already been calculated during the forward step, work backwards simulating each previous state in turn using (1).

## 2.2 Adaptive random walk Metropolis algorithm

Consider a  $d$ -dimensional target distribution  $\pi(\beta)$ . The *random walk Metropolis* algorithm (RWM) considers a local jump  $\epsilon$  drawn from a symmetric random jump proposal density  $g(\epsilon)$ ; in this article we consider the Gaussian distribution,  $\epsilon \sim N(\mathbf{0}, \Sigma)$ . The algorithm starts at  $\beta^{(0)} = (\beta_1^{(0)}, \beta_2^{(0)}, \dots, \beta_d^{(0)})$  and at time  $t + 1$  given  $\beta^{(t)}$ , we draw  $\epsilon$  and set  $\beta' = \beta^{(t)} + \epsilon$ . We accept or reject according to acceptance probability

$$\alpha = \min \left\{ 1, \pi(\beta') / \pi(\beta^{(t)}) \right\}.$$

If the proposal is accepted then  $\beta^{(t+1)} \leftarrow \beta'$ ; otherwise  $\beta^{(t+1)} \leftarrow \beta^{(t)}$ .

The efficiency of a given RWM algorithm depends heavily on the choice of  $\Sigma$ . Both Roberts and Rosenthal (2001) and Sherlock, Fearnhead and Roberts (2010) suggest that a RWM algorithm might achieve near optimal efficiency when  $\Sigma$  correctly represents the general shape of the target distribution, for example if it is proportional to the variance of  $\beta$  or the inverse curvature at the mode. The constant of proportionality should be adjusted so that the acceptance rate is approximately 23%.

Sherlock, Fearnhead and Roberts (2010) describes an *adaptive RWM* algorithm where, at the  $n$ th iteration, the jump is sampled from a mixture distribution:

$$\epsilon = \begin{cases} N(\mathbf{0}, m_n^2 \tilde{\Sigma}_n) & \text{with probability } 1 - \delta, \\ N(\mathbf{0}, m_0^2 \Sigma_0) & \text{with probability } \delta, \end{cases} \quad (2)$$

Here  $\delta$  is a small positive constant,  $\Sigma_0$  is a fixed covariance matrix and  $m_0 = 2.38/d^{1/2}$ , where  $d$  is the dimension of  $\beta$ . The matrix  $\tilde{\Sigma}_n$  is the estimated variance of  $\beta$  using the sample from the Markov chain to date. The scaling factor  $m_n$  for the adaptive part is initialized to  $m_0$ . If iteration  $n$  is from the non-adaptive part, then  $m_{n+1} \leftarrow m_n$ ; otherwise:

- if the proposal is rejected, then  $m_{n+1} \leftarrow m_n - \Delta/n^{1/2}$ .
- if the proposal is accepted, then  $m_{n+1} \leftarrow m_n + 3\Delta/n^{1/2}$ ,

where the adaptation quantity  $\Delta := m_0/100$ . These updates lead to an equilibrium acceptance rate of 25%.

The algorithm therefore adapts the proposal according to the information currently available about the posterior distribution. The fixed mixture component with (small) probability,  $\delta$ , is required to break the potential positive feedback where the proposal might adapt too well to a particular unimportant and unrepresentative part of the posterior and therefore continue to explore that portion and become less and less able to explore the main part of the posterior.

A similar algorithm is used in Roberts and Rosenthal (2010); the only difference being that  $m_n$  is fixed at a theoretically derived quantity.

### 3 Modelling the hidden and missing data

#### 3.1 Hidden Markov models for the diseases

Our analysis aims to explore the potential interactions described in 1.4 among the six diseases recorded in our data set. We could model each disease mathematically by a two-state discrete-time Markov chain, where state 1 corresponds to no disease and state 2 to presence of disease. This two-state model imposes a very specific structure. For example the length of any infection is geometrically distributed; however cowpox, for example, is known to last for approximately one month (Bennett *et al.* (1997), Chantrey (1999)). It has also been found (e.g. Telfer *et al.* (2010)) that the effect of a disease  $D_1$  on the probability of a vole contracting disease  $D_2$  can be different if the infection with  $D_1$  is in its first month (an acute phase) or in subsequent months (a chronic phase). In this analysis, the state space of some of the Markov chains is therefore extended to three or four states, where appropriate, in order to be able to adequately model the dynamics and influence of each disease.

For each transition probability we have a logistic regression model; for example the probability,  $p_{11}^{(t)}$ , that a given vole will be in state 1 (no disease) at time  $t + 1$  given that it is in state 1 at time  $t$  is given by

$$\text{logit}(p_{11}^{(t)}) = \mathbf{x}_t^T \beta_{11}.$$



Here  $\mathbf{x}_t$  is the vector of covariates at time  $t$ , which for all models includes the states of other diseases at time  $t$ , **time** (as a continuous covariate) in the format of lunar month, a seasonal cycle in the form of **seasin** and **seacos**, **sex**, **weight**, **site** and the interaction between **sex** and seasonal cycle. The model for cowpox also includes as covariates a different trend with lunar month for each site.

The remainder of this section gives a brief description of each disease in the study and describes the Markov model that is used to describe it. All transition probabilities are time dependent since some of the covariates are time-dependent; however for ease of notation we drop any explicit reference to this time dependence. A more detailed description of the host resources required by these parasites and a discussion about host immune responses can be found in Telfer *et al.* (2008).

### 3.1.1 *Bartonella* species

*Bartonella* is a genus of bacteria that infects mammals (including humans), usually transmitted by arthropods. The species investigated here are transmitted by fleas (Bown, Bennett and Begon (2004)). There are no grounds for assuming that the effect of other diseases and covariates on the probability that a vole will recover from a particular *Bartonella* species after the second (third fourth etc.) lunar month is different from the effect after the first month. However, since the majority of *Bartonella* infections last for one month and only a few last more than two (Birtles *et al.* (2001), Telfer *et al.* (2008)) the overall probabilities of recovering after the first and second month are likely to be different. Additionally a vole's chance of contracting a particular *Bartonella* species for the first time might be different from the chance of contracting it again after recovery from it in the past, although again, there is no reason to assume that the effects of other diseases and covariates on this are likely to be different. This suggests that each *Bartonella* species be modelled using a Markov chain with four states: 1=no infection, 2=new infection, 3=old infection, 4=uninfected but has had a past infection. The time-inhomogeneous transition probability matrix from time  $t$  to time  $t + 1$  for this Markov chain is

$$P = \begin{bmatrix} 1 - p_{12} & p_{12} & 0 & 0 \\ 0 & 0 & 1 - p_{24} & p_{24} \\ 0 & 0 & 1 - p_{34} & p_{34} \\ 0 & p_{42} & 0 & 1 - p_{42} \end{bmatrix}.$$

Each transition probability is governed by a logistic regression as follows:

$$\begin{aligned} \text{logit}(p_{12}) &= \beta_{0,12} + \mathbf{x}_{\text{contract}}^T \boldsymbol{\beta}_{\text{contract}}, \\ \text{logit}(p_{24}) &= \beta_{0,24} + \mathbf{x}_{\text{recover}}^T \boldsymbol{\beta}_{\text{recover}}, \\ \text{logit}(p_{34}) &= \beta_{0,34} + \mathbf{x}_{\text{recover}}^T \boldsymbol{\beta}_{\text{recover}}, \\ \text{logit}(p_{42}) &= \beta_{0,42} + \mathbf{x}_{\text{contract}}^T \boldsymbol{\beta}_{\text{contract}}. \end{aligned}$$

Here  $\mathbf{x}_{\text{recover}}$  and  $\mathbf{x}_{\text{contract}}$  depend on the states of the other species of *Bartonella*, on cowpox, *Babesia* and *Anaplasma* at the current time  $t$  as well as

on the vole’s weight at this time, on its site, sex, the seasonal covariates and on the interaction between sex and seasonal cycle. As justified above, we use the same vector covariates  $\mathbf{x}_{contract}$  and vector of covariate effects  $\beta_{contract}$  for the two probabilities related to contracting the particular *Bartonella* species. Similarly we use the same vectors covariates and covariate effects for the two probabilities relating to recovery from the disease,  $\mathbf{x}_{recover}$ ; we allow only the intercepts to differ. This assumption prevents a further increase in the, already large, number of parameters to be estimated.

### 3.1.2 *Babesia*

*Babesia microti* can cause haemolytic anaemia in infected hosts. It is a chronic infection, which is to say that once a host is infected it is never again free of the disease. The effect of a *Babesia* infection on the probabilities of contracting or recovering from one of the other diseases may depend on whether the *Babesia* infection is in its acute (in its first month) or chronic phase.

We therefore model *Babesia* using a Markov chain with the following three states: 1=no infection, 2=acute infection, 3=chronic infection. The transition matrix is

$$P = \begin{bmatrix} 1 - p_{12} & p_{12} & 0 \\ 0 & 0 & 1 \\ 0 & 0 & 1 \end{bmatrix}.$$

A logistic regression relates  $p_{12}$  to the covariates, including the states of the other diseases.

### 3.1.3 *Anaplasma*

*Anaplasma phagocytophilum* is a tick-borne bacterium that causes the disease granulocytic ehrlichiosis in humans. In the dataset there are relatively few positive records for *Anaplasma* and thus little power to ascertain transition probabilities and covariate effects from a third state of, for example, “currently uninfected but was previously infected”. Therefore, we use a two-state Markov chain with the following transition probability matrix

$$P = \begin{bmatrix} 1 - p_{12} & p_{12} \\ p_{21} & 1 - p_{21} \end{bmatrix}.$$

Separate logistic regressions relate  $p_{12}$  and  $p_{21}$  to the covariates, including the states of the other diseases.

### 3.1.4 Cowpox

In voles and other wild rodents, infection with cowpox virus lasts approximately 4 weeks (Bennett *et al.* (1997)). The diagnostic test, however, detects antibodies to the virus, not the virus itself. Antibodies appear approximately 2 weeks after contracting the infection but then remain present in the blood stream of a vole for the rest of its life (Bennett *et al.* (1997)). We therefore model

the progression as a Markov chain with three states: 1=never been infected, 2=infected, 3=infected in the past. The form of the transition matrix and the relationship between the states and the response, the presence or absence of antibodies to cowpox, is identical to that for *Babesia*. Naturally the coefficients of and, potentially, the covariate set for the logistic regression for  $p_{12}$  are different.

### 3.2 Other missing values

As mentioned in Section 1.4, for many voles not all of the covariates are available. For a given vole, the covariates `sex`, `site`, and `time` clearly carry over to the missing records. The unobserved disease states will be treated dynamically and will be sampled from the conditional distribution as part of the Gibbs sampling scheme (see Section 4.2). Such sampling could perhaps also be performed for `weight` if a satisfactory transition model could be found. However here we adopt a simpler approach whereby each missing weight value is imputed once via linear interpolation between the two nearest observed values for that vole. The robustness of inference to other sensible imputed weight values is investigated in Section 5.3.

## 4 Bayesian approach

### 4.1 Priors for the initial disease state of each Markov chain

This section describes the approach that we used to obtain the initial probability distribution,  $\boldsymbol{\pi}$ , of each unobserved Markov chain, as required by the forward-backward algorithm, as well as the priors for some of the parameters.

#### 4.1.1 Initial probability distribution

The forward-backward algorithm of Section 2.1 requires, for each vole and each disease, the distribution,  $\boldsymbol{\pi}$ , of the Markov chain on the set of states for that disease at the the first observation time for that vole. Our time-inhomogeneous Markov chains admit no limiting distribution and so the popular choice of setting the initial distribution to the limiting distribution of the chain is not available to us.

In the interest of simplicity we choose to estimate a single  $\boldsymbol{\pi}$  for each disease, by counting the proportion of times we believe a vole to be in each of the disease states. We describe the approach for the construction of  $\boldsymbol{\pi}$  for each *Bartonella* spp. in detail, as for the remaining diseases the construction is relatively straightforward.

Consider the observed disease state at time  $t$ ,  $D_t$ . If this is  $P$  then the state of the Markov chain,  $S_t$  is either 2 (new infection) or 3 (old infection). So that we can always distinguish between these states we only include observations on a given vole if the disease state of the same vole at the previous lunar month,  $D_{t-1}$ , was also observed. Observations with missing observations either side,

Table 2: Construction of states of the Markov chain.  $D_t$  is the current infection state,  $D_{t-1}$  is the previous infection state,  $D_h$  is the infection history and  $S_t$  is the current state of the Markov chain; here \* denotes that the entry is irrelevant.

$D_h$	$D_{t-1}$	$D_t$	$S_t$
N	N	N	1
*	N	P	2
*	P	P	3
*	P	N	4
P	N	N	4

such as  $xPx$ , are therefore ignored, and each set of  $n$  consecutive observations ( $n > 2$ ) therefore provides  $n - 1$  disease states. If  $D_t = N$  and at some time prior to  $t$  the vole was observed to be positive then we can be sure that  $S_t = 4$ . Complete disease profiles, since birth, are not available for any vole so that the lack of any observed positive in the vole’s history does not necessarily imply that a vole with  $D_t = N$  has  $S_t = 1$ . Nonetheless we choose to make this implication; we examine the robustness of inference to this choice in Section 5.3. As with the rest of this analysis we assume that the disease state of a vole at a given time is independent of whether or not that vole is caught at that time (see Section 1.3).

These rules are summarized in Table 2 where  $D_h$  represents a vole’s history prior to  $t - 1$  and is  $P$  if this history includes at least one positive, and is  $N$  otherwise (even if the history contains no observations).

Since no other dataset is available in which individual *Bartonella* spp. are identified, we employ this algorithm on the dataset which we are analysing. However, a similar longitudinal dataset to the one that we analyse was also available to us. This additional dataset arises from an earlier, three year study which was conducted using the same sampling design, but where the response for *Bartonella* was a single indicator for presence and absence, rather than an indicator for each species. Thus we use this dataset to estimate prior state probabilities for *Anaplasma*, *Babesia* and cowpox. As the Markov chain for *Anaplasma* has two states, estimation of the initial distribution is straightforward. For *Babesia* and cowpox we use a similar algorithm to *Bartonella*, but a simpler as their Markov chains have only three states.

#### 4.1.2 Prior distributions for the regression parameters

Using the covariate sets chosen for our main dataset we fitted a logistic regression to a subset of the additional dataset along the same lines as described in Section 1.3. Parameter estimates from these analyses were used to inform our choice of prior for similar parameters in our main analysis.

Since the additional dataset does not distinguish the *Bartonella* species, there is not an exact correspondence between parameters from the simple analyses and the parameters in our main model, and some of the parameters in our

main model have no counterpart in the simple analyses. All priors in our main analysis are independent and Gaussian. Where parameters do approximately correspond, we set the prior mean for the parameter in our main analysis to the MLE for the corresponding parameter in the simple analysis of the additional dataset, and the prior standard deviation to be three times the standard error of the MLE. Where no corresponding MLE exists, the parameter in our main analysis is given a vague but proper Gaussian prior.

## 4.2 Adaptive Metropolis-within-Gibbs algorithm

In our dataset, the target parameter,  $\beta$ , can be naturally partitioned into six sub-blocks, one for each disease. We therefore generalize the algorithm of Sherlock, Fearnhead and Roberts (2010) that was described in Section 2.2 to an *adaptive Metropolis-within-Gibbs* algorithm on  $k$  sub-blocks.

Let  $\beta = (\beta_1, \beta_2, \dots, \beta_k)$ , where  $\beta_i$  is the parameter set for the  $i$ th sub-block. Starting from the initial value  $\beta^{(0)} = (\beta_1^{(0)}, \beta_2^{(0)}, \dots, \beta_k^{(0)})$ , a single iteration cycles through all the sub-blocks updating each in turn and finishing with  $\beta = (\beta'_1, \beta'_2, \dots, \beta'_k)'$ . In the update for the  $i$ th block the current and proposed values are respectively:

$$\begin{aligned}\beta &:= \beta'_1, \dots, \beta'_{i-1}, \beta_i, \beta_{i+1}, \dots, \beta_k, \\ \beta^* &:= \beta'_1, \dots, \beta'_{i-1}, \beta_i + \epsilon, \beta_{i+1}, \dots, \beta_k.\end{aligned}\tag{3}$$

Here the proposal jump  $\epsilon$  in (3) for the  $i$ th sub-block at the  $n$ th iteration is sampled from the mixture distribution in (2). Naturally we allow different covariance matrices and scaling factors for each of the sub-blocks, i.e.  $m_{n,i}$ ,  $\tilde{\Sigma}_{n,i}$ ,  $m_{0,i}$  and  $\Sigma_{0,i}$  for  $i = 1, \dots, k$ ; also  $d$  is now the dimension of the  $i$ th sub-block.

As we have already mentioned, our target of interest is the joint posterior distribution of the coefficients of the logistic regressions for the transition probabilities in Section 3.1. We simulate from the joint posterior distribution of these coefficients and the hidden disease states with the following MCMC algorithm.

Let the chain at the  $i$ th iteration be  $\beta^{(i)} = (\beta_1^{(i)}, \beta_2^{(i)}, \dots, \beta_6^{(i)})$ , where the  $j$ th block comprises of the  $\beta$ 's of the logistic regressions for the  $j$ th disease ( $j = 1, \dots, 6$ ). Each step of the Gibbs sampler is as follows.

- Simulate from  $\beta_1^{(i)} | Y_1, X_2^{(i-1)}, \dots, X_6^{(i-1)}$  through an adaptive RWM step.
- Simulate the hidden states for the first disease from  $X_1^{(i)} | \beta_1^{(i)}, Y_1, X_2^{(i-1)}, \dots, X_6^{(i-1)}$  using the forward-backward algorithm.
- Simulate from  $\beta_2^{(i)} | X_1^{(i)}, Y_2, X_3^{(i-1)}, \dots, X_6^{(i-1)}$  through an adaptive RWM step.
- Simulate the hidden states for the second disease from  $X_2^{(i)} | X_1^{(i)}, \beta_2^{(i)}, Y_2, X_3^{(i-1)}, \dots, X_6^{(i-1)}$  using the forward-backward algorithm.

- ...
- Simulate from  $\beta_6^{(i)} | X_1^{(i)}, X_2^{(i)}, \dots, X_5^{(i)}, Y_6$ .
- Simulate  $X_6^{(i)} | X_1^{(i)}, X_2^{(i)}, \dots, X_5^{(i)}, \beta_6^{(i)}, Y_6$ ,

where  $X_j$  is the simulated unobserved Markov chain of the disease  $j$ .

### 4.3 Algorithm implementation and details

Consider the  $v^{th}$  vole,  $v = 1, \dots, V$ . Let  $\mathbf{y}_T^{(v)} = (y_1^{(v)}, y_2^{(v)}, \dots, y_{T_v}^{(v)})$  be the observed sequence for a particular disease for the  $v^{th}$  vole. This sequence takes the values 0 and 1, indicating negative and positive status in a disease respectively. We consider in detail the implementation for any species of *Bartonella* since the specifics for each of other diseases can be considered as a special case of this.

As described in Section 3.1 the underlying unobserved Markov chain  $\{X_t\}$  for the *Bartonella* species has a state space of cardinality 4 and takes the following values: 1=no disease, 2=new infection, 3=old infection and 4=not having the disease but had it in the past. As a result, an observation of  $y_i = 0$  corresponds to hidden process of  $X_i = 1$  or  $X_i = 4$ , and an observation of  $y_i = 1$  corresponds to  $X_i = 2$  or  $X_i = 3$ . In the implementation of the forward-backward algorithm (Section 2.1) the likelihood vector is

$$\mathbf{l}^{(t)}(y) = (1 - y, y, y, 1 - y), \quad y = 0, 1.$$

If the observation at time  $t$  is missing we set  $\mathbf{l}^{(t)}(y) = (1, 1, 1, 1)$ .

The adaptive algorithm described in 4.2 requires the fixed covariance matrix  $\Sigma_0$ . For each disease, a separate non-adaptive RWM was performed for the logistic regressions coefficients associated with the hidden Markov model for this disease that are not associated with the other diseases; for example weight and sex. The block of  $\Sigma_0$  associated with these covariates was estimated directly from this run. Each of the remaining  $\beta$  coefficients was given a small variance in  $\Sigma_0$  and was assumed to be uncorrelated with any of the other coefficients. Also to ensure a sensible non-singular  $\hat{\Sigma}_n$ , for each disease, proposals from the adaptive part were only allowed once at least 1000 proposed jumps had been accepted. We set  $\delta = 0.1$ . All of the computationally intensive parts of the algorithm were coded in C within an R wrapper.

## 5 Analysis and results

### 5.1 Convergence of the algorithm

Three independent Markov chains of length 300,000 were generated from the algorithm in Section 4.2; each chain was started from a different position. Six of 235 traceplots from one of the chains are reproduced in Figure 2. In the first two of the six traceplots the first few tens of thousands of the iterations

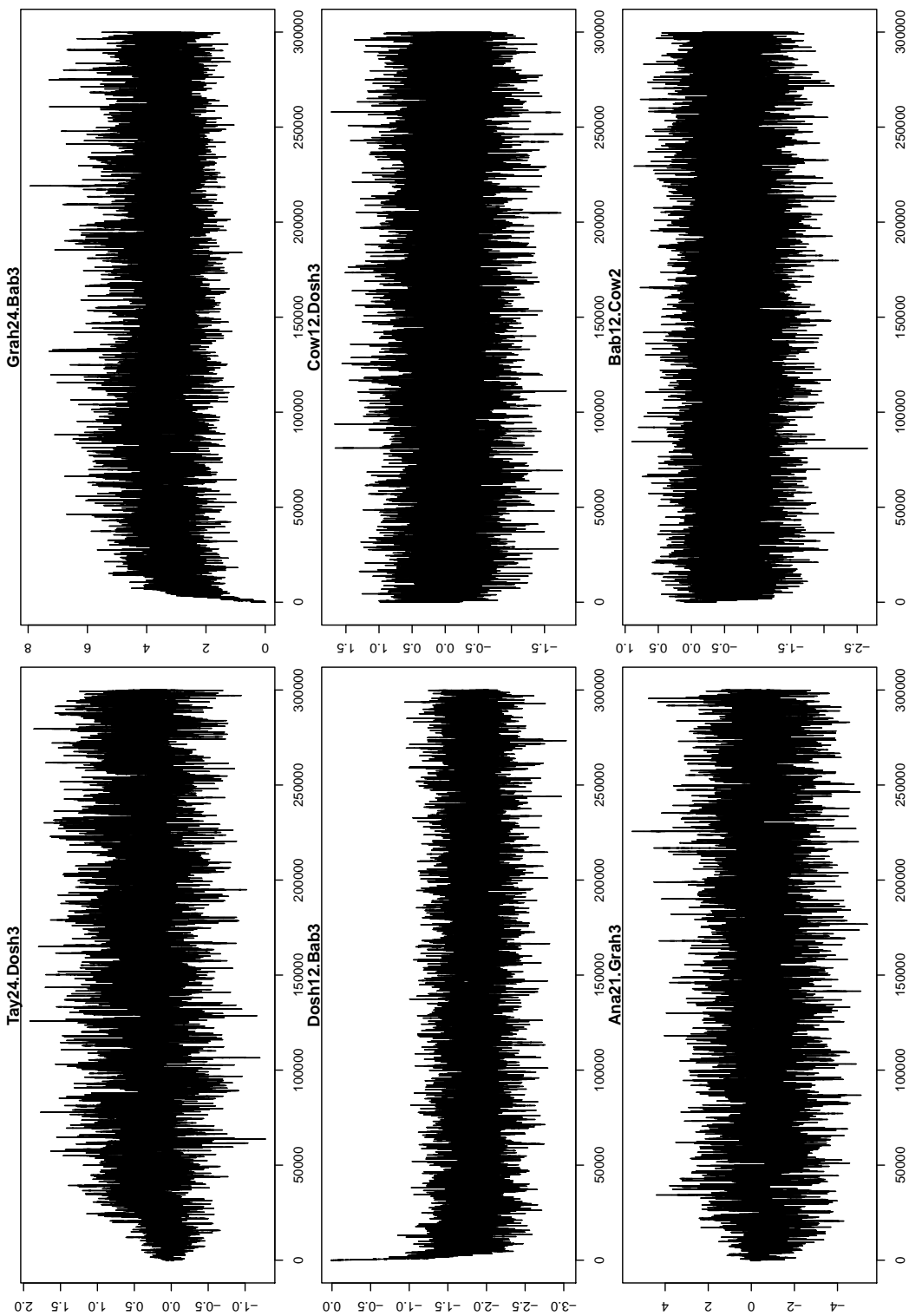


Figure 2: Six of the 235 traceplots for the first of the three runs of the Markov chain. Each traceplot represents the  $\beta$  coefficient of the logistic regression for the transition probabilities of the HMM for a different disease.

show the variance of the proposal increasing as the adaptive algorithm learns the shape of the posterior; this was the case in many of the 235 traceplots.

The Gelman-Rubin statistic (Gelman and Rubin (1992)),  $R$ , was calculated from the three chains for each of the 235 components of  $\beta$ . Figure 3 shows the mean of the estimated  $R$  statistics and the maximum of the estimated  $R$  statistics, plotted against iteration number. The plot suggests that a burn-in period of 100,000 iterations should be more than sufficient. Inference is performed using the final 200,000 iterations from each of the 3 runs combined.

## 5.2 Posterior inference

We are interested in interactions between diseases, for example in whether or not presence or absence of disease  $D_1$  affects the probability of a change of state for disease  $D_2$ . In each logistic regression for each transition matrix, we therefore examine the coefficients that correspond to the states of the other diseases. We are also interested (for *Bartonella*) in whether or not the status of an infection (new or old) affects the chance of recovery, and in whether or not a previous infection affects the chance of a new infection with the same species; these correspond respectively to the contrasts:  $\beta_{0,34} - \beta_{0,24}$  and  $\beta_{0,42} - \beta_{0,12}$ .

Formal model choice, for example via reversible jump MCMC (?), is computationally infeasible here. Instead we take a high posterior probability that a given parameter or contrast is positive (or a high probability that it is negative) as indicating a potential interaction. For an individual parameter we might consider  $P(\text{positive}) > 0.975$  or  $P(\text{positive}) < 0.025$  as indicating a likely interaction. We are however interested in a total of 116 parameters and contrasts which raises a similar problem to that of multiple testing in classical statistics. Whilst considering probabilities below 0.025 or above 0.975 to indicate a possible interaction, we therefore take probabilities below 0.00025 and above 0.99975 as indicating a very probable interaction.

Table 3 shows those parameters for which the posterior probability of positivity is either above 0.975 or below 0.025. The table shows the posterior median, a 95% credibility interval, and the posterior probability that the parameter is positive.

Firstly, and most clearly, the presence of *Babesia* decreases the probability of contracting *Bartonella* and increases the probability of recovery from *Bartonella*. This is true for both chronic and acute *Babesia* infections and for all three species of *Bartonella*. There is no evidence for the reverse interaction, that is for the presence of *Bartonella* affecting the chance of contracting *Babesia*.

For two of the three *Bartonella* species (*B. taylorii* and *B. grahamii*) a vole is more likely to recover from an old infection than a new one and is less likely to be re-infected following previous exposure. Furthermore, a vole that has recovered from a *B. taylorii* infection is less likely to contract *B. grahamii*. In addition, there seems to be a decrease in the probability of contracting *B. doshiae* when a vole has been exposed to *B. taylorii* whether or not it is still infected. Finally, infection with *Anaplasma* appears to increase the probability of recovery from *B. grahamii*; there was some evidence for the same interaction



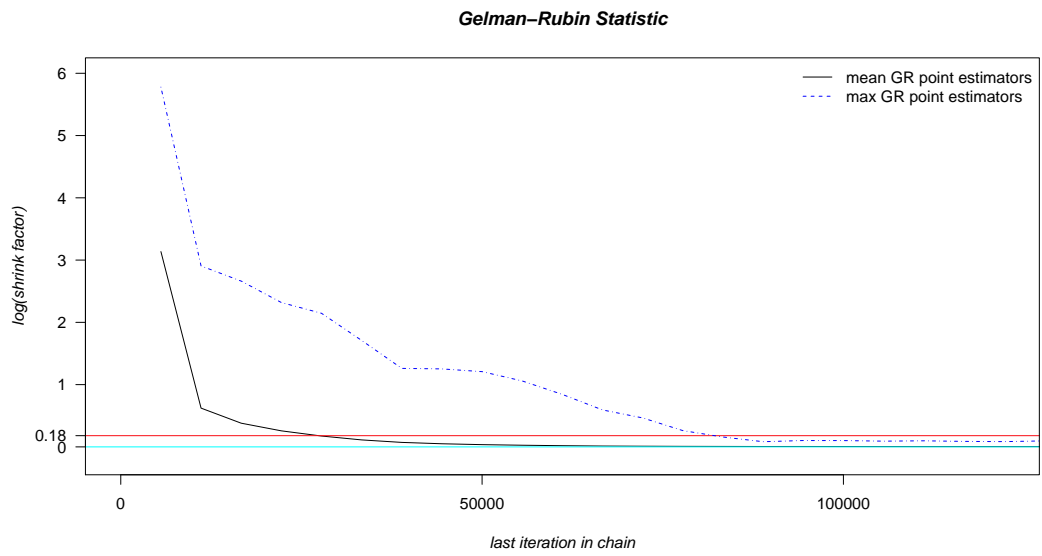


Figure 3: Combined Gelman-Rubin statistics for all 235  $\beta$ 's;  $R_1, \dots, R_{235}$ . Black:  $\frac{1}{235} \sum_i R_i$ ; blue:  $\max_i R_i$ . Statistics are plotted on the log scale against iteration number. The light blue line indicates ideal ratio of  $\log(1)$  and red line the threshold of  $\log(1.2)$  suggested in Gelman (1996).

with *B. doshiae* with posterior probability 0.956. There is no evidence of a change to the probability of recovery from *B. taylorii* (probability= 0.347). It is also possible that a current infection with cowpox virus hinders recovery from *B. doshiae*.

### 5.3 Sensitivity analysis

Three somewhat arbitrary choices were made in the set up of our model and priors: the interpolation scheme that fills in missing weight values, the choice of prior distribution for the state of the hidden Markov model for a particular disease and vole, and the exact relationship between parameters estimated in the simple analysis of the alternative dataset and priors for parameters in the hidden Markov models for the main dataset.

An alternative for each of these choices is described below. For each alternative three further chains of length 300,000 were created and checked for convergence. Then any sizeable changes in the conclusions that would be drawn from the posterior distributions of the parameters were noted.

In the main analysis, missing weight values were filled in via linear interpolation. As an alternative we considered the logistic growth curve which was proposed in Burthe *et al.* (2009). We assumed Gaussian residuals for the logarithm of weight and allowed the logistic growth parameters to depend on covariates such as the sex of the vole and the time of year; some of the coefficients were also allowed to include subject specific random effects. More details are provided in Xifara (2012).

In the main analysis the prior distribution for the state of the hidden Markov model for each *Bartonella* species was estimated from the dataset as detailed in Table 2. However some of the observations that were allocated to state 1 could in fact have corresponded to state 4; we therefore calculate an alternative prior,  $\pi^*$  for each *Bartonella* species from the prior used in the main analysis:  $\pi^* = (\frac{1}{2}\pi_1, \pi_2, \pi_3, \frac{1}{2}\pi_1 + \pi_4)$ . For the main analysis, prior distributions for the hidden Markov models for cowpox, *Anaplasma* and *Babesia* were calculated from the additional data set detailed in Section 4.1.1. For the alternative analysis we estimate these priors from the main dataset.

In the main analysis, where there was a rough correspondence between a parameter in the simple analysis of the alternative dataset and one in the main analysis, we centered the Gaussian prior in the main analysis on the maximum likelihood estimate from the simple analysis and set the standard deviation to be three times the estimated standard error from the simple analysis (Section 4.1.2). As an alternative we use vague but proper Gaussian priors for all parameters.

Parameter estimates with the alternative weight scheme or with the alternative priors for parameters were very similar to the estimates from the main set-up. For all the significant covariates none of the posterior probabilities changed by more than 0.005. However, the change to the prior distribution of the hidden states affected three of the twenty one covariates in table 3. In particular, the effects on a vole’s probability of contracting *B. doshiae* when the vole was infected (old infection) or currently uninfected but infected in the

Table 3: Posterior summaries of model parameters of interest for which the probability of positivity is either above 0.975 or below 0.025. For each parameter the posterior median and a 95% credibility interval is provided, as well as the probability that the parameter is greater than zero. Each parameter arises from a logistic regression coefficient for a particular transition probability in the hidden Markov model for a particular disease. The disease and transition appear in the first part of the coefficient's name. The second part of the name is separated from the first by a dot and indicates the particular disease that is influencing the transition probability and the state of this disease. State 1 is always taken to be the baseline. The contrasts  $X_{.42.0-12.0}$  and  $X_{.34.0-24.0}$  are defined in Section 5.2.

<i>Covariate</i>	<i>Median</i>	<i>95% CI</i>	<i>Posterior Probability</i>
dosh12.tay3	-0.7304	(-1.4279,-0.0593)	0.0165
dosh12.tay4	-0.6454	(-1.2065,-0.0866)	0.013
dosh12.bab2	-1.4716	(-2.4395,-0.6839)	0.0001
dosh12.bab3	-1.7457	(-2.2191,-1.3108)	0
dosh24.bab2	2.8513	(1.4697,4.551)	1
dosh24.bab3	3.4399	(2.0126,5.4971)	1
dosh24.cow2	-1.3534	(-2.6362,-0.202)	0.0106
grah12.tay4	-0.6858	(-1.1516,-0.2311)	0.0019
grah12.bab2	-1.1919	(-2.0261,-0.4617)	0.0004
grah12.bab3	-1.8316	(-2.358,-1.3492)	0
grah42.0-12.0	-1.1342	(-2.0051,-0.0955)	0.0173
grah24.bab2	2.8385	(1.2861,5.1721)	1
grah24.bab3	1.9865	(1.0646,3.0964)	1
grah24.ana2	1.2353	(0.1682,2.4308)	0.9894
grah34.0-24.0	0.7935	(0.0149,1.6006)	0.9772
tay12.bab2	-1.3891	(-2.2791,-0.5985)	0.0001
tay12.bab3	-1.4028	(-1.8917,-0.9643)	0
tay42.0-12.0	-2.4984	(-3.6459,-1.1622)	0.0008
tay24.bab2	1.6973	(0.6862,2.8488)	0.9996
tay24.bab3	1.818	(1.1346,2.5935)	1
tay34.0-24.0	1.2191	(0.5546,1.9186)	0.9999

past by *B. taylorii* became apparently unimportant, with posterior probabilities changing from 0.0165 to 0.109 and from 0.013 to 0.108, respectively. Also the posterior probability that the difference in recovery from an old infection and a new infection with *B. grahamii* to be greater than zero decreased by 0.01. No additional covariates became important in any of the three alternative runs.

## 6 Discussion

We have described a discrete-time hidden Markov model for interactions between diseases in a host and used it to analyse data from a longitudinal study of field voles with records of six different pathogens. Inference is possible despite the relatively large fraction of missing data and is performed via a Gibbs sampler that cycles through the diseases, alternately sampling from the hidden states for that disease and then from the parameters for the transition probabilities in the Markov model for that disease. An adaptive random walk Metropolis-within-Gibbs algorithm learns about the posterior distribution as it proceeds and aids efficient exploration of the high-dimensional statespace. The Markov model offers a more detailed description than the existing modelling approach and the inference methodology that we introduce is able to use more of the data than the existing standard inference methodology.

Our original dataset consists of 4771 captures of 2072 voles. The simple analysis, described in Section 1.3, only looks at transitions from an N. For *B. taylorii* and *Babesia*, for example, (1200, 920) such transitions on (667, 508) voles are examined. In contrast our analysis examined (1807, 1344) transitions from an N on (938, 623) voles. Moreover, our analysis looks at both transitions from an N and transitions from a P.

We now examine the most major findings of Section 5.2 and briefly discuss the biological insights that they offer. For two of the *Bartonella* species, voles are more likely to recover from an old infection than a new one, which is to be expected given that more complete histories for individuals indicate that most infections last for only one month. Previous data also indicate that *B. doshiae* infections may last longer than *B. taylorii* and *B. grahamii* infections (Telfer *et al.* (2007)). Also, for two species, previous infection by a species appears to grant some form of immunity to that species, suggesting that hosts can develop an effective acquired immune response. To date, there has been conflicting evidence for such a response in wild populations, suggesting immune responses may vary between host species and/or *Bartonella* species (Birtles *et al.* (2001), Kosoy *et al.* (2004), Bai *et al.* (2011)). Interestingly also *B. taylorii* infection appears to provide immune cross-protection to *B. grahamii* and *B. doshiae* infection.

We found, for voles currently infected with *Babesia*, both a reduction in susceptibility to *Bartonella* and an increase in the probability of recovery from *Bartonella* over the next lunar month. We also found no evidence that a current *Bartonella* infection might influence susceptibility to *Babesia* over the next month. Telfer *et al.* (2010) use a similar logistic regression strategy to that

detailed in Section 1.3; however one of the differences is that they allow both the current ( $t_0$ ) and future ( $t_1$ ) state of each disease covariate to influence the probability that, for the disease that is being treated as a response, a vole is positive at time  $t_1$  given that it is negative at time  $t_0$ . Both our simple analyses and our full HMM methodology only allow covariates at time  $t_0$ . Telfer *et al.* (2010) find the *Babesia* covariates, both at time  $t_0$  and  $t_1$ , to be significant for predicting the probability of catching *Bartonella* between  $t_0$  and  $t_1$ . The *Bartonella* covariate at time  $t_1$  is also found to be significant in predicting susceptibility to *Babesia*, apparently contradicting our findings. We show in the Appendix, however, that assuming only the negative effects of *Babesia* on *Bartonella* infections detected in this study, and no other dependency between *Bartonella* and *Babesia*, is sufficient to lead to a negative correlation between *Bartonella* and *Babesia* at any given time. Since the effect of *Babesia* on *Bartonella* is so pronounced (Table 3), it is certainly believable that this negative correlation could be strong enough that each of the two diseases at  $t_1$  is an important covariate for the other.

Our methodology provides a substantial extension to that of Pradel (2005). We allow for multiple (here six) hidden Markov models, and we allow the transition probabilities to depend on covariates via logistic regressions. Moreover the hidden Markov models are fitted jointly, with the (unknown) state of each model acting as a covariate for the change of state probabilities for all other diseases. In the application which we have considered, missingness was believed to be independent of disease state; in other scenarios, such as those considered in Pradel (2005) the probability that a given subject will be observed might depend on the states of each of the hidden Markov models. This could be accommodated within our methodology through a further logistic regression for the probability of being observed given the set of hidden states and other covariate information, and several other minor changes as detailed in Pradel (2005).

## 7 Appendix

Let us assume, as we found, that

$$P(Bart_{t_1} = 1 | Bab_{t_0} = 1, Bart_{t_0} = 0) < P(Bart_{t_1} = 1 | Bab_{t_0} = 0, Bart_{t_0} = 0) \quad (4)$$

$$P(Bart_{t_1} = 1 | Bab_{t_0} = 1, Bart_{t_0} = 1) < P(Bart_{t_1} = 1 | Bab_{t_0} = 0, Bart_{t_0} = 1) \quad (5)$$

Let us also assume that status of *Bartonella* at  $t_0$  does not influence susceptibility to *Babesia* at  $t_1$ , since we found no evidence against this.

$$P(Bab_{t_1} = 1 | Bab_{t_0}, Bart_{t_0}) = P(Bab_{t_1} = 1 | Bab_{t_0}) \quad (6)$$

Finally we assume that, conditional on the disease states at  $t_0$ , the states of *Bartonella* and *Babesia* at  $t_1$  are independent.

$$P(Bab_{t_1}, Bart_{t_1} | Bab_{t_0}, Bart_{t_0}) = P(Bab_{t_1} | Bab_{t_0}, Bart_{t_0}) P(Bart_{t_1} | Bab_{t_0}, Bart_{t_0}) \quad (7)$$

Given Equations (4) and (5) we can also write

$$P(\text{Bart}_{t_1} = 1 | \text{Bab}_{t_0} = 1) < P(\text{Bart}_{t_1} = 1 | \text{Bab}_{t_0} = 0). \quad (8)$$

Equations (6) and (7) imply conditional independence just given the status of *Babesia*

$$P(\text{Bab}_{t_1}, \text{Bart}_{t_1} | \text{Bab}_{t_0}) = P(\text{Bab}_{t_1} | \text{Bab}_{t_0})P(\text{Bart}_{t_1} | \text{Bab}_{t_0}). \quad (9)$$

Since the left hand side is

$$P(\text{Bab}_{t_1} | \text{Bab}_{t_0}, \text{Bart}_{t_0} = 0)P(\text{Bab}_{t_1} | \text{Bab}_{t_0}, \text{Bart}_{t_0} = 0) + P(\text{Bab}_{t_1} | \text{Bab}_{t_0}, \text{Bart}_{t_0} = 0) = \\ P(\text{Bab}_{t_1} | \text{Bab}_{t_0}, \text{Bart}_{t_0} = 1) \{P(\text{Bab}_{t_1} | \text{Bab}_{t_0}, \text{Bart}_{t_0} = 0) + P(\text{Bart}_{t_1} | \text{Bab}_{t_0}, \text{Bart}_{t_0} = 1)\}$$

which is equal to the right hand side.

Finally, note that  $P(\text{Bab}_{t_1} = 1 | \text{Bab}_{t_0} = 1) = 1$  and use Proposition 7.1 (below) to find

$$P(\text{Bab}_{t_1} = 1, \text{Bart}_{t_1} = 1) - P(\text{Bab}_{t_1} = 1)P(\text{Bart}_{t_1} = 1) = \\ p(1-p) \{P(\text{Bart}_{t_1} | \text{Bab}_{t_0} = 1) - P(\text{Bart}_{t_1} = 1 | \text{Bab}_{t_0} = 0)\} \{1 - P(\text{Bab}_{t_1} = 1 | \text{Bab}_{t_0} = 0)\},$$

where  $p = P(\text{Bab}_{t_0} = 1)$ . Equation (8) implies that the first term in square brackets is negative. Hence the presence of *Babesia* and *Bartonella* at any given time,  $t_1$ , are negatively correlated.

**Proposition 7.1.** *Let the variables  $X, Y$  to be conditionally independent given the binary variable  $Z \in \{0, 1\}$ . Then*

$$P(X, Y) - P(X)P(Y) = p(1-p) \{P(Y|Z = 1) - P(Y|Z = 0)\} \{P(X|Z = 1) - P(X|Z = 0)\},$$

where  $p = P(Z = 1)$ .

*Proof.* By the law of total probability and since  $X, Y$  are conditionally independent we can write

$$P(X, Y) = p \cdot P(X|Z = 1)P(Y|Z = 1) + (1-p) \cdot P(X|Z = 0)P(Y|Z = 0). \quad (10)$$

Now,

$$P(X) = p \cdot P(X|Z = 1) + (1-p) \cdot P(X|Z = 0) \\ P(Y) = p \cdot P(Y|Z = 1) + (1-p) \cdot P(Y|Z = 0)$$

So,

$$P(X)P(Y) = p^2 P(X|Z = 1)P(Y|Z = 1) + p(1-p) \cdot P(X|Z = 1)P(Y|Z = 0) \\ + p(1-p)P(X|Z = 0)P(Y|Z = 1) + (1-p)^2 P(X|Z = 0)P(Y|Z = 0)$$

Thus,

$$P(X, Y) - P(X)P(Y) = p(1-p)P(X|Z = 0)P(Y|Z = 0) + p(1-p)P(X|Z = 1)P(Y|Z = 1) \\ - p(1-p)P(X|Z = 0)P(Y|Z = 1) - p(1-p)P(X|Z = 1)P(Y|Z = 0) \\ = p(1-p) \{P(Y|Z = 1) - P(Y|Z = 0)\} \{P(X|Z = 1) - P(X|Z = 0)\}.$$

□

## Acknowledgements

Part of this work was funded through North West Development Agency project number N0003235. The second author acknowledges also financial support from the Engineering and Physical Sciences Research Council and the Faculty of Science and Technology at Lancaster University. The field work was supported by funding from the Natural Environment Research Council (GR3/13051) and The Wellcome Trust (075202/Z/04/Z; 070675/Z/03/Z).

## References

- Bai, Y., Calisher, C.H., Kosoy, M.Y., Root, J.J. and Doty, J.B. (2011) Persistent infection or successive reinfection of deer mice with *Bartonella vinsonii* subsp. *arupensis*. *Applied and Environmental Microbiology*, **77**, 1728–1731.
- Baum, I. E., Petrie, Y., Soules, G. and Weiss, N. (1970) A maximisation technique occurring in the statistical analysis of probabilistic functions of Markov chains. *The Annals of Mathematical Statistics*, **41**, 164–171.
- Begon, M., Telfer, S., Burthe, S. J., Lambin, X., Smith, J. M. and Paterson, S. (2009) Effects of abundance on infection in natural populations: Field voles and cowpox virus. *Epidemics*, **1**, 35–46.
- Bennett, M., Crouch, A.J., Begon, M., Duffy B., Feore S., Gaskell, R. M., Kelly, D. F., McCracken, C. M., Vicaryw, L. and Baxby, D. (1997) Cowpox in British voles and mice. *Journal of Comparative Pathology*, **116**, 35–44.
- Birtles, R. J., Hazel, S. M., Bennett, M., Bown, K., Raoult, D. and Begon, M. (2001) Longitudinal monitoring of the dynamics of infections due to *Bartonella* species in UK woodland rodents. *Epidemiology and Infection*, **126**, 323–329.
- Burthe, S.J., Telfer, S., Begon, M., Bennett, M., Smith A. and Lambin, X. (2008) Cowpox virus infection in natural field vole, *Microtus agrestis*, populations: significant negative impacts on survival. *Journal of Animal Ecology*, **77**, 110–119.
- Burthe, S. J., Lambin, X., Telfer, S., Douglas, A., Beldomenico, P., Smith, A. and Begon, M. (2009) Individual growth rates in natural field voles, *Microtus agrestis*, populations exhibiting cyclic population dynamics. *Oecologia*, **162**, 653–661.
- Bown, K. J, Bennett, M. and Begon, M. (2004) Flea-borne *Bartonella grahamii* and *Bartonella taylorii* in Bank Voles. *Emerging Infectious Diseases*, **10**, 684–687.
- Bown, K. J., Lambin, X., Telford, G. R., Ogden, N. H., Telfer, S., Woldehiwet, Z. and Birtles, R. J. (2008) Relative Importance of *Ixodes ricinus* and *Ixodes*

- trianguliceps* as Vectors for *Anaplasma phagocytophilum* and *Babesia microti* in Field Vole (*Microtus agrestis*) Populations. *Appl. Environ. Microbiol.*, **74**, 7118–7125.
- Chantrey, J. (1999) *The epidemiology of cowpox in its reservoir hosts*. PhD Thesis, University of Liverpool, Liverpool, UK.
- Chantrey, J., Meyer, H., Baxby, D., Begon, M., Bown, K. J., Hazel S. M., Jones, T., Montgomery, W. I. and Bennett, M. (1999) Cowpox: reservoir hosts and geographic range. *Epidemiol. Infect.*, **122**, 455–460.
- Courtney, J. W. L., Kostelnik, M., Zeidner, N. S. and Massung, R. F. (2004) Multiplex real-time PCR for detection of *Anaplasma phagocytophilum* and *Borrelia burgdorferi*. *J. Clin. Microbiol.*, **42**, 3164–3168.
- Daniels, M. J. and Hogan, J. W. (2008) *Missing Data in Longitudinal Data: Strategies for Bayesian Modelling and Sensitivity Analysis*. Chapman & Hall/CRC. Monographs on Statistics & Applied Probability.
- Gelman, A. (1996) *Markov Chain Monte Carlo in Practice*, chap. Inference and monitoring convergence. Chapman & Hall/CRC.
- Gelman, A. and Rubin, D. (1992) Inference from iterative simulation using multiple sequences. *Statistical Science*, **7**, 457–472.
- Geman, A. and Geman, D. (1984) Stochastic relaxation, Gibbs distribution and the Bayesian restoration of images. *Journal of Applied Statistics*, **20**, 25–62.
- Gilks, W., Richardson, S. and Spiegelhalter, D. (1996) *Markov chain Monte Carlo in Practice*. Chapman & Hall/CRC.
- Gilks, W., Roberts, G. O. and Sahu, S. (1998) Adaptive Markov chain Monte Carlo through regeneration. *Journal of the American Statistical Association*, **93**, 1045–1054.
- Kosoy, M., Mandel, E., Green, D., Marston, E. and Childs, J. (2004). Prospective studies of *Bartonella* of rodents. Part I. Demographic and temporal patterns in population dynamics. *Vector-Borne Zoonotic Diseases*, **4**, 285–295.
- Lindley, D. V. (1980) Approximate Bayesian Methods. *Bayesian Statistics*, Valenthia, 223–237.
- Lachish, S., Knowles, S.C.L., Alves, R., Wood, M.J. and Sheldon, B.C. Infection dynamics of endemic malaria in a wild bird population: parasite species-dependent drivers of spatial and temporal variation in transmission rates. *Journal of Animal Ecology*, **80**, 1207–1216.
- Metropolis, N., Rosenbluth, A., Rosenbluth, M., Teller, A. and Teller, E. (1953) Equation of state calculations by fast computing machines. *Journal of Chemical Physics*, **21**, 1087–1091.



- Neals, P. and Roberts, G. O. (2006) Optimal scaling for partially updating mcmc algorithms. *Annals of Applied Probability*, **16**, 475–515.
- Pawitan, Y. (2001) *In All Likelihood: Statistical Modelling and Inference Using Likelihood*. Oxford University Press Inc., New York.
- Pradel, R. (2005) Multievent: an extension of multistate capture-recapture models to uncertain states. *Biometrics*, **61**, 442–447.
- Roberts, G. O. and Rosenthal, J. (2001) Optimal scaling for various Metropolis-Hastings algorithms. *Statistical Science*, **16**, 351–367.
- Roberts, G. O. and Rosenthal, J. (2010) Examples of adaptive MCMC. *J. Comp. Graph. Stat.*, **8**, 349–367.
- Scott, S. L. (2002) Bayesian methods for hidden Markov models: Recursive computing in the 21th century. *Journal of the American Statistical Association*, **97**, 337–351.
- Sherlock, C., Fearnhead, P. and Roberts, G. O. (2010) The random walk Metropolis: Linking theory and practice through a case study. *Statistical Science*, **28**, 172–190.
- Telfer, S., Begon, M., Bennett, M., Bown, K., Burthe, S., Lambin, X., Telford, G. and Birtles, R. (2007) Contrasting Dynamics of *Bartonella* spp. in Cyclic Field Vole populations: the Impact of Vector and Host Dynamics. *Parasitology* **134**, 413–425.
- Telfer, S., Birtles, R., Bennett, M., Lambin, X., Paterson, S. and Begon, M. (2008) Parasite interactions in natural populations: insights from longitudinal data. *Parasitology*, **135**, 767–781.
- Telfer, S., Lambin, X., Birtles, R., Beldomenico, P., Burthe, S. J., Paterson, S. and Begon, M. (2010) Species interactions in a parasite community drive infection risk in a wildlife population. *Science*, **330**, 243–246.
- Xifara T. D. (2012) Technical Report.